

Strong-coupling limit in the evolution from BCS superconductivity to Bose-Einstein condensation

P. Pieri* and G. C. Strinati†

Dipartimento di Matematica e Fisica, Sezione INFM, Università di Camerino, I-62032 Camerino, Italy

(Received 22 December 1999)

We consider the problem of the crossover from BCS superconductivity to Bose-Einstein condensation in three dimensions for a system of fermions with a mutual attractive interaction, for which we adopt the simplifying assumption of a suitably regularized point-contact interaction. We examine in a critical way the fermionic (self-consistent) T -matrix approximation, which has been widely utilized in the literature to describe this crossover *above* the superconducting critical temperature, and show that it fails to yield the correct behavior of the system in the strong-coupling limit, where composite bosons form as tightly bound fermion pairs. We then set up the correct approximation for a “dilute” system of composite bosons and show that a class of diagrams has to be considered in the place of the fermionic T -matrix approximation for the self-energy. This class of diagrams correctly describes *both* the weak- and strong-coupling limits, and consequently results in an improved interpolation scheme for the intermediate (crossover) region. In this context, we provide also a systematic mapping between the corresponding diagrammatic theories for the composite bosons and the constituent fermions. As a preliminary result to demonstrate the numerical effect of our class of diagrams on physical quantities, we calculate the value of the scattering length for composite bosons in the strong-coupling limit and show that it is considerably modified with respect to the result obtained within the self-consistent fermionic T -matrix approximation.

I. INTRODUCTION

The problem of the crossover from BCS superconductivity to Bose-Einstein (BE) condensation has attracted considerable interest lately,¹ and especially after the recent angle-resolved photoemission spectroscopy experiments in cuprate superconductors which have shown the existence of a (pseudo) gap at temperatures above the superconducting transition temperature T_c .^{2,3} This observation has prompted the proposal by many authors of the possible presence of quasibound fermionic pairs *above* T_c and up to a second temperature scale T^* .

From the theoretical point of view, this crossover problem (as well as related crossover problems, like the one associated with the Mott transition⁴) poses a compelling challenge, because approximations that are valid on the one side of the crossover are not necessarily valid on the opposite side. In addition, the crossover region is characterized (or even defined) by the absence of a “small” parameter, which would allow one to control the approximations. For systems that are sufficiently “dilute” (such that, for instance, for a given strength of the interparticle interaction, the density ρ can be taken to be arbitrarily small), one could directly exploit the well-known results obtained for “dilute” fermionic systems with $\rho_F = \rho$, on the one hand,⁵ or for “dilute” bosonic systems with $\rho_B = \rho/2$, on the other hand,⁶ to get a correct description of the limits on the two sides of the crossover.

For a “dilute” fermionic system the two-body equation plays an essential role.⁵ In particular, in three dimensions the low-energy two-body scattering process can be parametrized in terms of the *scattering length* a_F , which is negative for weak coupling and positive for strong coupling (i.e., in the presence of a bound state for the attractive interaction), and diverges when the coupling strength suffices for the bound state to appear. For strong coupling, a_F gives the size of the

bound state. The many-body approach to a “dilute” fermionic system then relies on the identification of the many-body T matrix with a_F , which, in the repulsive case, is always possible in the low-density limit. The classification of diagrams is thus made in terms of the small parameter $k_F a_F$ (where k_F is the Fermi wave vector of the noninteracting system). In the case of interest to us of an *attractive* interaction, however, past the critical interaction strength where the two-body problem develops a bound state, the many-body T matrix *acquires a singularity* (pole) for all interaction strengths and no identification of the T matrix with a_F is clearly possible any longer. The smallness of the parameter $k_F a_F$ *both* in the weak- and strong-coupling limit⁷ might not, therefore, be sufficient to guarantee that an approximation selected for the weak-coupling limit is still valid in the strong-coupling limit.

In particular, the T -matrix approximation for the fermionic self-energy (which has invariably been regarded in the literature as representing *the* dilute-approach approximation to the BCS-BE crossover problem)^{7–12} is *not* expected to remain valid as soon as the two-body bound state develops. This statement is consistent with the physical picture that, *as soon as the two-body bound state develops, it is the residual interaction between the composite bosons to determine the “diluteness” condition of the system* and not the original attraction between the constituent fermions which produces the bound state to begin with and relatively to which the system is in the strong-coupling limit.¹³ It is then clear that a correct description of the strong-coupling limit can be obtained only by selecting the relevant approximations directly for a *dilute system of composite bosons*, rather than relying on the fermionic T -matrix approximation, which is valid by construction for a *dilute system of fermions*.

From previous work on the functional-integral approach

to the crossover from BCS to BE,^{14–16} one knows that approximations (like the BCS mean field at zero temperature), which give a satisfactory account of the weak-coupling limit, become inadequate in the strong-coupling limit, and that only when including fluctuation corrections at least at the one-loop level a sensible description of the effective bosonic system in the strong-coupling limit results. This remark has actually suggested that the crossover problem should be dealt with *in reverse*,¹⁵ that is, by first envisaging approximations which give a satisfactory description of the strong-coupling (bosonic) limit and by extrapolating them toward the weak-coupling (fermionic) limit, where they are expected to work properly as well.¹⁷

One then anticipates the set of many-body (self-energy) diagrams, which describe the bosonic limit, to be much richer than the corresponding set of diagrams which describe the fermionic limit. In fact, from the previous discussion we do *not* expect the fermionic T -matrix approximation to be appropriate for describing the “dilute” bosonic limit properly. We will indeed show below that the fermionic T -matrix approximation corresponds in the strong-coupling limit to the standard bosonic Hartree-Fock approximation, and that, for this reason, it misses all but one of the infinite set of self-energy diagrams associated with a “dilute” bosonic system.¹⁸

In this paper, we present the formal theory for the choice of the fermionic self-energy diagrams starting from the strong-coupling side, for temperatures *above* T_c (in the sense that no anomalous single-particle fermionic propagator will be considered) and for three spatial dimensions. The corresponding theory below T_c , as well as in lower spatial dimensions, remains to be developed. An extensive numerical study based on this approximation is under way and will be discussed separately. The only numerical calculation presented in this paper concerns the value of the composite-boson scattering length a_B in the strong-coupling limit.

The plan of the paper is as follows. In Sec. II we discuss some introductory material, which is necessary for setting up our “low-density” approximation for composite bosons. Specifically: We introduce a suitable regularization for the fermionic point-contact interaction, which allows us to select readily the relevant classes of fermionic diagrams; We summarize the mapping onto a bosonic system in the strong-coupling limit, obtained by the procedure of Ref. 15; We discuss the standard fermionic T -matrix approximation and show how the Hartree-Fock approximation for composite bosons results from it in the strong-coupling limit. In Sec. III, we introduce the theory of the “low-density” Bose gas for composite bosons and obtain the fermionic self-energy from the bosonic self-energy in the “low-density” approximation. In Sec. IV we present the numerical calculation for the composite-boson scattering length a_B in the strong-coupling limit and discuss the physical implications of our result. Section V gives our conclusions.

II. BUILDING BLOCKS OF THE DIAGRAMMATIC STRUCTURE FOR COMPOSITE BOSONS

In this section we discuss the diagrammatic structure that generically describes the composite bosons in terms of the constituent fermions, as a preliminary step for setting up the

“low-density” approximation for composite bosons in the next section. Our construction rests on a judicious choice of the fermionic interaction, which (albeit without loss of generality) greatly reduces the number and considerably simplifies the expressions of the Feynman diagrams to be taken into account.

A. Regularization of the fermionic interaction

We begin by considering the following simple model Hamiltonian for interacting fermions (we set Planck \hbar and Boltzmann k_B constants equal to unity throughout):

$$H = \sum_{\sigma} \int d\mathbf{r} \psi_{\sigma}^{\dagger}(\mathbf{r}) \left(-\frac{\nabla^2}{2m} - \mu \right) \psi_{\sigma}(\mathbf{r}) + \frac{1}{2} \sum_{\sigma, \sigma'} \int d\mathbf{r} d\mathbf{r}' \psi_{\sigma}^{\dagger}(\mathbf{r}) \psi_{\sigma'}^{\dagger}(\mathbf{r}') \times V_{\text{eff}}(\mathbf{r} - \mathbf{r}') \psi_{\sigma'}(\mathbf{r}') \psi_{\sigma}(\mathbf{r}), \quad (2.1)$$

where $\psi_{\sigma}(\mathbf{r})$ is the fermionic field operator with spin projection $\sigma = (\uparrow, \downarrow)$, m is the fermionic (effective) mass, μ is the fermionic chemical potential, and $V_{\text{eff}}(\mathbf{r} - \mathbf{r}')$ is an *effective potential* that provides the *attraction* between fermions. To simplify the ensuing many-body diagrammatic structure considerably (and yet preserving the physical effects we are after), we adopt for V_{eff} the simple form of a “contact” potential¹⁹

$$V_{\text{eff}}(\mathbf{r} - \mathbf{r}') = v_0 \delta(\mathbf{r} - \mathbf{r}'), \quad (2.2)$$

where v_0 is a negative constant. With this choice, the interaction affects only fermions with opposite spins in the Hamiltonian (2.1) owing to the Pauli principle. A suitable *regularization* of the potential (2.2) is, however, required to get accurate control of the many-body diagrammatic structure. In particular, the equation (in the center-of-mass frame)

$$\frac{m}{4\pi a_F} = \frac{1}{v_0} + \int \frac{d\mathbf{k}}{(2\pi)^3} \frac{m}{\mathbf{k}^2} \quad (2.3)$$

for the *fermionic scattering length* a_F associated with the potential (2.2) is ill defined, since the integral over the three-dimensional wave vector \mathbf{k} is ultraviolet divergent. The δ -function potential (2.2) is then effectively regularized, by introducing an ultraviolet cutoff k_0 in the integral of Eq. (2.3) and letting $v_0 \rightarrow 0$ as $k_0 \rightarrow \infty$, in order to keep a_F fixed at a chosen *finite* value. The required relation between v_0 and k_0 is obtained directly from Eq. (2.3). One finds

$$v_0 = -\frac{2\pi^2}{mk_0} - \frac{\pi^3}{ma_F k_0^2} \quad (2.4)$$

when $k_0 |a_F| \gg 1$. With the regularization (2.4) for the potential, the classification of the many-body diagrams gets considerably simplified, since only specific substructures of these diagrams survive when the limit $k_0 \rightarrow \infty$ is eventually taken. In particular, in order to obtain a finite result for a given Feynman diagram, the vanishing strength of the potential v_0 should be compensated by an ultraviolet divergence in some internal momentum integration. Two examples of alternative behaviors are given in Figs. 1(a) and 1(b). For the particle-particle ladder of Fig. 1(a) the internal momentum

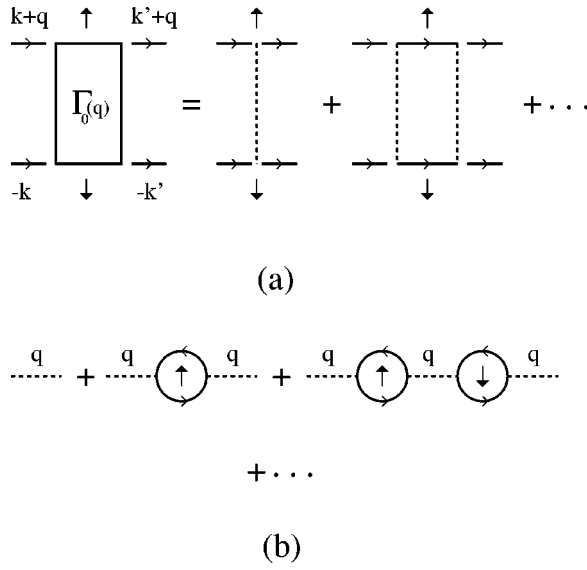


FIG. 1. (a) Particle-particle ladder and (b) series of particle-hole bubbles. Note that for a point-contact potential the particle-particle ladder depends only on the sum of the incoming (outgoing) four momenta. Four momenta are indicated and spin labels are represented by up and down arrows.

integration associated to every rung is divergent in the limit $k_0 \rightarrow \infty$ and compensates the vanishing v_0 , yielding the finite result:

$$\Gamma_0(q) = - \left\{ \frac{m}{4\pi a_F} + \int \frac{d\mathbf{k}}{(2\pi)^3} \times \left[\frac{\tanh[\beta\xi(\mathbf{k})/2] + \tanh[\beta\xi(\mathbf{k}-\mathbf{q})/2]}{2[\xi(\mathbf{k}) + \xi(\mathbf{k}-\mathbf{q}) - i\Omega_\nu]} - \frac{m}{\mathbf{k}^2} \right] \right\}^{-1}, \quad (2.5)$$

where $\xi(\mathbf{k}) = \mathbf{k}^2/(2m) - \mu$. For the particle-hole bubble series of Fig. 1(b) we obtain instead a vanishing result, since, in this case, the internal momentum integration is cut off by the Fermi factors and thus converges. In an analogous way, one can show that in the particle-particle channel the contributions of the vertex corrections and of the two-particle effective interactions other than the rung vanish for our choice of the potential, since they both contain a factor of the particle-hole type.

It is thus evident from these considerations that, with our choice of the fermionic interaction, the *skeleton structure* of the diagrammatic theory can be constructed only with the particle-particle ladder (2.5) plus an infinite number of interaction vertices, like the ones depicted in Fig. 2 (besides *one* spare single-particle fermionic Green's function that enters the fermionic self-energy diagrams, which in turn contains, in principle, all self-energy insertions originating from self-consistency). The ladder and the vertices of Fig. 2 contain, by construction, only "bare" single-particle fermionic Green's functions. These vertices serve to connect the ladders among themselves, thus generating complex diagrammatic structures. In analogy with the so-called Hikami vertices occurring in the weak-localization problem,²⁰ we refer to these vertices as the four, six, ..., n -point vertices, in the order.

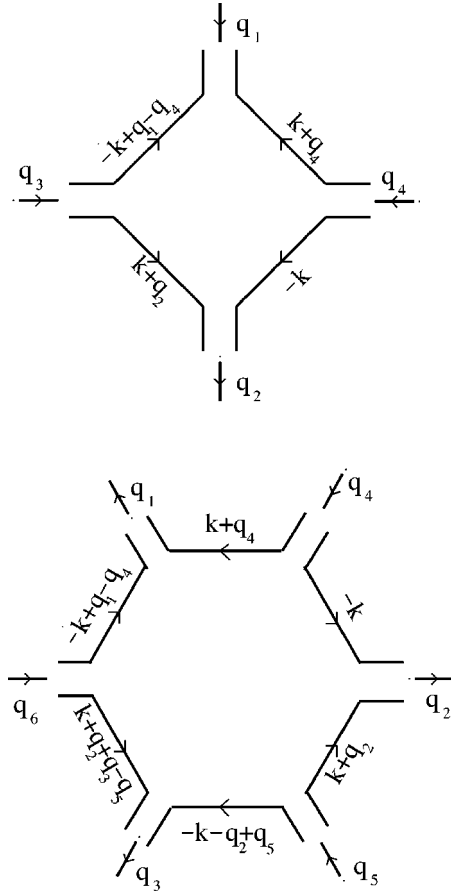


FIG. 2. Four- and six-point vertices for composite bosons. Incoming and outgoing bosonic four momenta are indicated, as well as four momenta on each fermionic line. Spin labels are understood to alternate on successive fermionic lines.

As far as the dressing of the particle-particle ladder is concerned, the above statements can be justified in a rigorous fashion by resorting, e.g., to functional-integral methods. Before going to consider such functional-integral methods it is, however, important to examine in detail the analytic behavior of our building block $\Gamma_0(q)$ in the weak- and strong-coupling limits.²¹

In the weak-coupling limit, one readily obtains to lowest order in $k_F a_F$:

$$\Gamma_0(q) \approx - \frac{4\pi a_F}{m}, \quad (2.6)$$

which allows us to classify the diagrammatic structure in powers of $k_F a_F$. In the strong-coupling limit (whereby $\beta\mu \rightarrow -\infty$),²¹ on the other hand, the particle-particle ladder $\Gamma_0(q)$ has the following *polar structure*:⁷

$$\Gamma_0(q) \approx - \frac{4\pi}{m^2 a_F} \frac{1 + \sqrt{1 + \left(-i\Omega_\nu + \frac{\mathbf{q}^2}{4m} - \mu_B \right) \epsilon_0^{-1}}}{i\Omega_\nu - \left(\frac{\mathbf{q}^2}{4m} - \mu_B \right)}, \quad (2.7)$$

where we have used the definition $\mu_B = 2\mu + \epsilon_0$ for the bosonic chemical potential ($\epsilon_0 = 1/(ma_F^2)$ being the bound-state energy of the two-body problem). Note that (apart from

the residue being different from unity) the expression (2.7) resembles a “free” boson propagator with Matsubara frequency Ω_ν (ν integer), wave vector \mathbf{q} , and mass $2m$. It is thus evident that the classification of diagrams developed for a “dilute” system in weak coupling (which relies on the finite value (2.6) of the particle-particle ladder—cf. Ref. 5) can no longer be utilized in the strong-coupling limit, since in this case the particle-particle ladder does not reduce to a constant but develops a polar structure [cf. Eq. (2.7)]. *In the strong-coupling limit, a different classification scheme is therefore required to organize the diagrammatic structure for a “dilute” system.* This point was not properly realized by previous work on the BCS to BE crossover and especially by the work of Ref. 7, where the “diluteness” condition of the system was explicitly assumed both in the weak- and strong-coupling limit.

B. Mapping onto a bosonic system via functional integrals

We briefly review the procedure of Ref. 15 to extract the set of effective bosonic interactions mentioned above from the original fermionic action. By performing a Hubbard-Stratonovich transformation, the original fermionic partition function $\mathcal{Z} = \int \mathcal{D}\bar{c}\mathcal{D}c \exp\{-S\}$ was written in Ref. 15 as $\mathcal{Z} = \int \mathcal{D}b^*\mathcal{D}b \exp\{-S_{\text{eff}}\}$ in terms of bosonic variables, where the “effective” bosonic action can be expressed as a series expansion: $S_{\text{eff}} = \sum_{l=1}^{\infty} S_{\text{eff}}^{(2l)}$. The first term of this expansion is quadratic and reads

$$S_{\text{eff}}^{(2)} = \frac{\mathcal{V}}{\beta} \sum_{\mathbf{q}} |b(\mathbf{q})|^2 \Gamma_0^{-1}(\mathbf{q}), \quad (2.8)$$

where \mathcal{V} is the quantization volume. The “bare” bosonic propagator is thus expressed in terms of the particle-particle ladder (2.5), by writing

$$\langle b^*(\mathbf{q})b(\mathbf{q}) \rangle_{S_{\text{eff}}^{(2)}} = \frac{\beta}{\mathcal{V}} \Gamma_0(\mathbf{q}). \quad (2.9)$$

This identification is shown graphically in Fig. 3(a) for a definite choice of the spin labels (this convention will be maintained in the rest of the paper). It is important to emphasize that the identification (2.9) (as well as the other results of this subsection) holds *irrespective* of the value of the fermionic scattering length a_F . Nonetheless, referring to a system of interacting composite bosons acquires physical meaning in the strong-coupling limit only.

The *quartic* term in the expansion of S_{eff} is instead given by

$$S_{\text{eff}}^{(4)} = \frac{1}{4\beta\mathcal{V}} \sum_{q_1 \dots q_4} \tilde{u}_2(q_1 \dots q_4) b^*(q_1) b^*(q_2) b(q_3) b(q_4), \quad (2.10)$$

where the (four-point) *effective two-boson interaction* reads (cf. Fig. 2)

$$\begin{aligned} \tilde{u}_2(q_1 \dots q_4) &= \delta_{q_1+q_2, q_3+q_4} \left(\frac{\mathcal{V}}{\beta}\right)^2 \frac{2}{\beta\mathcal{V}} \sum_{\mathbf{k}} \\ &\times \frac{1}{\epsilon(-\mathbf{k})\epsilon(\mathbf{k}+q_2)\epsilon(-\mathbf{k}+q_1-q_4)\epsilon(\mathbf{k}+q_4)}. \end{aligned} \quad (2.11)$$

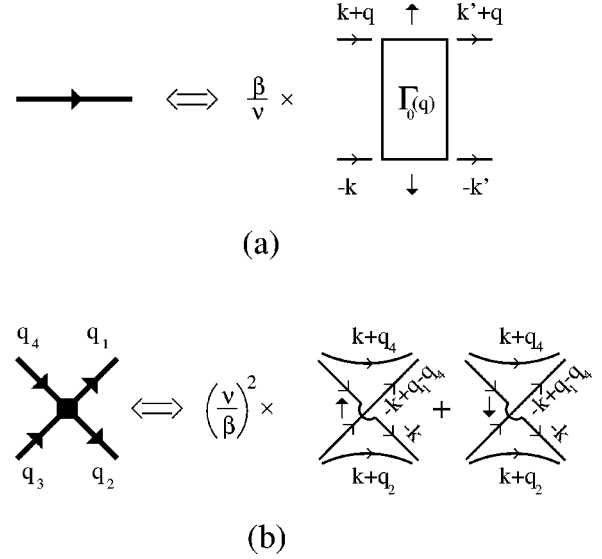


FIG. 3. Graphical correspondence (a) between the “bare” propagator for composite bosons (represented by a thick line) and the fermionic particle-particle ladder of Fig. 1(a), and (b) between the effective two-boson interaction and the four-point vertex of Fig. 2, where now the spin labels have been explicitly indicated in the internal lines. Note that the fermionic lines composing the four-point vertex have been rearranged with respect to Fig. 2, in order to resemble the bosonic vertex more closely (accordingly, the fermionic lines never intersect each other in the four-point vertex). Appropriate powers of β/\mathcal{V} as required by Eqs. (2.9) and (2.11) have been indicated explicitly.

It is worth noting the following features of the above expressions: (i) The interaction (2.11) depends on wave vectors *as well as* on Matsubara frequencies, revealing in this way the composite nature of the bosons; (ii) The energy denominators in Eq. (2.11) correspond to single-particle (bare) fermionic Green’s functions, since $\mathcal{G}^0(k) = \epsilon(k)^{-1}$; (iii) The factor of 2 in the definition (2.11) corresponds to the two different sequences of spin labels that can be attached to the four fermionic Green’s functions, as shown graphically in Fig. 3(b) (where the identification with the effective two-boson interaction is also indicated). Keeping track of the spin labels will, in fact, prove important in the following to establish the desired mapping between the bosonic and fermionic diagrammatic structures.

When considering the sum $S_{\text{eff}}^{(2)} + S_{\text{eff}}^{(4)}$ of the quadratic and quartic actions, the bosonic propagator $\langle b^*(\mathbf{q})b(\mathbf{q}) \rangle_{S_{\text{eff}}^{(2)} + S_{\text{eff}}^{(4)}}$ can be expressed in terms of the “bare” bosonic propagator (2.9) and of the effective two-boson interaction (2.11) via Wick’s theorem. The topology of the resulting diagrammatic structure, as well as the symmetry factor of each diagram, are identical to those obtained for true (point-like) bosons.^{22,23} The associated fermionic diagrammatic structure can then be constructed whenever needed by the correspondence rules shown in Fig. 3.

As an example of this correspondence, we show in Fig. 4 the bosonic propagator to first order in the interaction, together with the associated fermionic diagrams for the two-fermion Green’s function in the particle-particle channel. Note that the minus sign, which is associated with one power of the interaction in the bosonic diagram, is associated in-

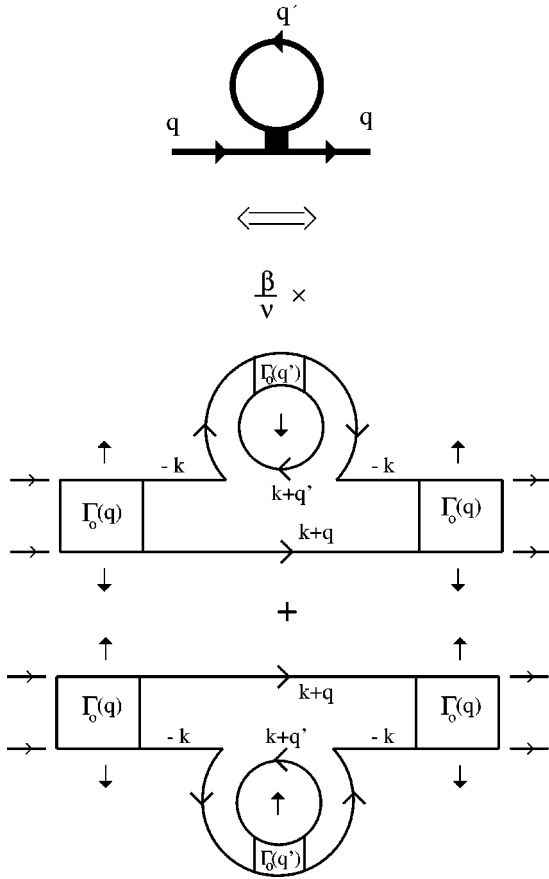


FIG. 4. Graphical correspondence between the composite-boson propagator and the two-fermion Green's function in the particle-particle channel, to first order in the *four-point* interaction vertex. This vertex can be identified from Fig. 2 by setting $q_2 = q_3 = q$ and $q_1 = q_4 = q'$ therein.

stead with the presence of a closed loop in the corresponding fermionic diagrams (the minus signs associated with the fermionic interaction being already taken into account in the definition of the particle-particle ladder). Note also that the bosonic self-energy insertion of Fig. 4 has the same topological structure of the bosonic Hartree-Fock self-energy diagram.

$$\begin{aligned} \tilde{u}_3(q_1 \dots q_6) &= \delta_{q_1+q_2+q_3, q_4+q_5+q_6} \left(\frac{\mathcal{V}}{\beta}\right)^3 \frac{2}{\beta\mathcal{V}} \sum_k \frac{(-1)}{\epsilon(-k)\epsilon(k+q_2)\epsilon(-k-q_2+q_5)} \\ &\times \frac{1}{\epsilon(k+q_2+q_3-q_5)\epsilon(-k+q_1-q_4)\epsilon(k+q_4)}. \end{aligned} \quad (2.15)$$

In the strong-coupling limit, whereby $|\mu|$ is the relevant energy scale in the problem, from dimensional considerations we get $\tilde{u}_2(\beta/\mathcal{V})^2 \sim |\mu|^{-3/2}$ and $\tilde{u}_3(\beta/\mathcal{V})^3 \sim |\mu|^{-7/2}$ (in three dimensions). For this reason, the contribution of the three-boson vertex (2.15) is suppressed with respect to the contribution of the two-boson vertex (2.11). To be more precise, one should compare the values of similar diagrams con-

A typical value of the two-boson effective interaction is obtained by considering the strong-coupling limit $\beta\mu \rightarrow -\infty$ and setting $q_1 = \dots = q_4 = 0$ in Eq. (2.11). One gets

$$\tilde{u}_2(0) = 2 \left(\frac{\mathcal{V}}{\beta}\right)^2 \left(\frac{m^2 a_F}{8\pi}\right)^2 u_2(0), \quad (2.12)$$

where¹⁵

$$u_2(0) = \frac{4\pi(2a_F)}{2m}. \quad (2.13)$$

The factor $m^2 a_F / (8\pi)$ in Eq. (2.12) reflects the difference between the true bosonic propagator and the particle-particle ladder in the strong-coupling limit [cf. also Eq. (2.7)]. Owing to this difference, $u_2(0)$ given by Eq. (2.13) [and not $\tilde{u}_2(0)$ given by Eq. (2.12)] has to be identified with the boson-boson interaction at zero four momenta. We return to the difference between \tilde{u}_2 and u_2 in Sec. III A.²⁴

Recalling further that the scattering length a_B^{Born} within the Born approximation, obtained for a pair of true bosons (each of mass $2m$) mutually interacting via a two-body potential with Fourier transform $u_2(0)$ at zero wave vector, is given by $a_B^{\text{Born}} = 2mu_2(0)/(4\pi)$, Eq. (2.13) yields the following relation between the bosonic and fermionic scattering lengths:

$$a_B^{\text{Born}} = 2a_F. \quad (2.14)$$

The result (2.14) was also obtained in Ref. 7 within the fermionic self-consistent *T*-matrix approximation (which corresponds to the bosonic Hartree-Fock approximation of Fig. 4 in the strong-coupling limit—see the next subsection), where it was erroneously regarded to be the value of the scattering length a_B for a “dilute” system of composite bosons. We will, in fact, show in Sec. IV that the result (2.14) actually differs from a_B , when *all* diagrams associated with a “dilute” system of composite bosons are taken into account.

Besides the four-point vertex (2.11), the composite nature of the bosons produces (an infinite set of) additional vertices. In particular, from the mapping of Ref. 15 we obtain the following expression for the six-point vertex (cf. Fig. 2):

structed with the four- and six-point vertices, respectively (like, for instance, the ones depicted in Figs. 4 and 5). The value of the diagram of Fig. 5 is smaller than the value of the diagram of Fig. 4 by the quantity

$$\frac{|\mu|^{-7/2} \epsilon_F^3 |\mu|}{|\mu|^{-3/2} \epsilon_F^{3/2} |\mu|^{1/2}} \sim (k_F a_F)^3. \quad (2.16)$$

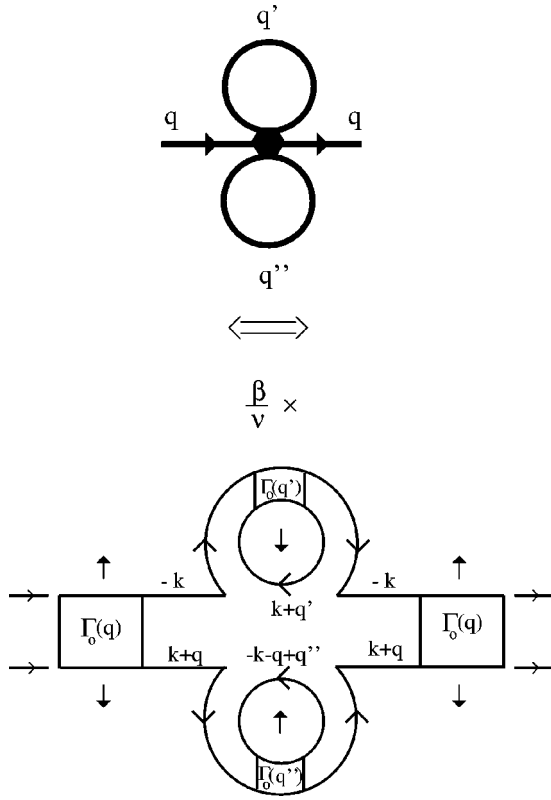


FIG. 5. Graphical correspondence between the composite-boson propagator and the two-fermion Green's function in the particle-particle channel, to first order in the *six-point* interaction vertex. This vertex can be identified from Fig. 2 by setting $q_2=q_6=q$, $q_1=q_4=q'$, and $q_3=q_5=q''$ therein.

Here, the factors containing the Fermi energy ϵ_F [$=k_F^2/(2m)=(3\pi^2\rho)^{2/3}/(2m)$] originate from the bosonic cycles (cf. Sec. III), while the factors $|\mu|$ and $|\mu|^{1/2}$ originate from the residue in Eq. (2.7). The diagram of Fig. 5 can thus be neglected in comparison to the diagram of Fig. 4, since $k_F a_F \ll 1$ in the strong-coupling limit.

The above argument can be made more general, by showing that *all interaction vertices can be neglected in comparison with the four-point vertex in the strong-coupling limit*.²⁵ In this limit, one can thus construct all diagrams representing the two-particle Green's function in the particle-particle channel in terms of the “bare” ladder and of the four-point interaction vertex only. This is precisely what one would expect on physical grounds, since the interactions involving more than two bodies become progressively less effective as the composite bosons overlap less when approaching the strong-coupling limit. In the next subsection we will show how the (self-consistent) fermionic T -matrix approximation can be examined in terms of the four, six, . . . , n -vertex functions in the strong-coupling limit.

C. Fermionic T -matrix approximation in the strong-coupling limit

The T -matrix approximation for a “dilute” Fermi gas represents one of the few cases in the many-body theory where the choice of the self-energy diagrams can be controlled by an external small parameter.²⁶ In the original version by Galitskii,⁵ the T -matrix approximation was con-

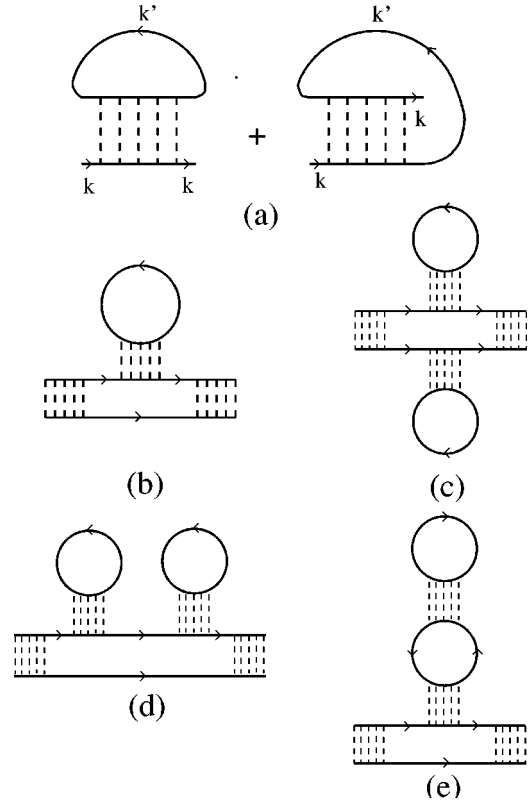


FIG. 6. (a) Self-energy diagrams corresponding to the self-consistent fermionic T -matrix approximation (full lines here represent self-consistent fermionic single-particle Green's functions and spin labels have been suppressed); Self-energy corrections entering the particle-particle ladder, obtained by contracting the (b) four-point vertex and (c)–(e) six-point vertex (full lines now represent the “bare” fermionic single-particle Green's functions).

ceived for a *repulsive* fermionic interaction of finite range (thus excluding bound states) and with the scattering length a_F always positive (albeit small). The fermionic self-energy diagram associated with this approximation is depicted at the left in Fig. 6(a), and is obtained by closing the particle-particle ladder with a single-particle Green's function in the only possible way. [The diagram at the right in Fig. 6(a) was included by Galitskii original treatment,⁵ but vanishes for our choice of the attractive potential since it contains forbidden interactions between parallel spins. By the same token, no spin summation needs to be considered for the fermionic loop at the left in Fig. 6(a).] In Fig. 6(a) all single-particle lines are regarded to be *self-consistent*, and thus contain self-energy insertions of the same kind of the ones depicted in the figure.²⁷ In this way, the self-consistent fermionic T matrix is “conserving” in the Baym-Kadanoff sense.^{28,29} Recalling that (with our regularization of the potential) the particle-particle ladder depends only on the sum of the incoming (outgoing) four-momenta, the self-energy of Fig. 6(a) reads

$$\Sigma_F(k) = -\frac{1}{\beta V} \sum_{k'} \Gamma_s(k+k') \mathcal{G}(k'), \quad (2.17)$$

where Γ_s is obtained from Γ_0 by replacing everywhere the “bare” \mathcal{G}_0 with the self-consistent \mathcal{G} .

By exploiting our diagrammatic correspondence rules, the self-energy insertions on Γ_0 can be interpreted in terms of

the four, six, . . . , -point interaction vertices discussed in the previous subsections. Typical examples are shown in Figs. 6(b)–6(e), where the “bare” single-particle lines associated with the vertices are marked by arrows. Note, in particular, that the diagram of Fig. 6(b) corresponds to a contraction of the four-point vertex, while the diagrams of Figs. 6(c)–6(e) correspond to all possible contractions of the six-point vertex. Additional diagrams not shown in the figure would then contain interaction vertices of higher order. Note also that the diagrams of Figs. 6(b)–6(c) have been already considered in Fig. 4 and in Fig. 5, respectively. From the results of the previous subsection we then conclude that only the diagram of Fig. 6(b) needs to be retained in the strong-coupling limit, the other diagrams being suppressed with respect to it at least by a factor $(k_F a_F)^3$ [cf. Eq. (2.16)]. The diagram of Fig. 6(b) corresponds to the Hartree-Fock approximation for the self-energy of composite bosons.¹⁸ Note finally that self-energy insertions on \mathcal{G}^0 in Eq. (2.17) could be interpreted similarly, in an open-ended way.

The above argument leads us to the conclusion that the fermionic T -matrix approximation reproduces the Hartree-Fock approximation to the self-energy of composite bosons in the strong-coupling limit. There exist, however, *additional* contributions to the self-energy of composite bosons which are of the *same order* (in the small parameter $k_F a_F$) of the Hartree-Fock approximation just discussed. These contributions are not included in the fermionic T -matrix approximation and must be considered separately, as discussed in the next section.

III. T -MATRIX APPROXIMATION FOR COMPOSITE BOSONS

In this section we set up an approximation for the fermionic self-energy, which describes the “low-density” regime *both* in the weak-coupling (fermionic) and in the strong-coupling (bosonic) limits on equal footing.

A. Low-density approximation for composite bosons

Before examining the “low-density” approximation for composite bosons, it is instructive to briefly recall some standard results concerning the self-energy for a “dilute” system of true (point-like) bosons. The argument to select the diagrams giving the leading contribution to the self-energy for a “low-density” Bose gas proceeds as follows.^{6,22,23} Let $u(\mathbf{q}_1, \mathbf{q}_2, \mathbf{q}_3, \mathbf{q}_4)$ be the (symmetrized) bosonic interaction potential, assumed to be vanishing for $|\mathbf{q}_i| \geq r_0^{-1}$ ($i = 1, \dots, 4$), where r_0 is the range of the potential. We shall also consider temperatures not much higher than the BE critical temperature, so that we shall assume $T \sim \rho^{2/3}$. Under these conditions, it turns out that *every cycle in a diagram contributes a factor $T^{3/2} \sim \rho$* .³⁰ The point is that factors $(e^{\beta \epsilon_B(\mathbf{q})} - 1)^{-1}$ arise after summation over the frequencies along the cycle. These factors cut off the integrals over the momentum variable for $|\mathbf{q}| \sim T^{1/2}$, which is of the order $\rho^{1/3}$ and much smaller than r_0^{-1} owing to the “diluteness” condition. It then follows that, for a “low-density” Bose system, the leading self-energy diagrams contain the *minimum number* of cycles, like the diagrams shown in Fig. 7(a), which constitutes the so-called bosonic T -matrix approximation.^{6,22,23}

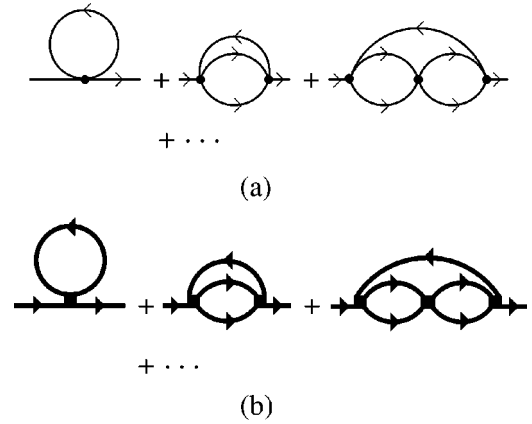


FIG. 7. (a) T -matrix approximation to the self-energy of true bosons; (b) T -matrix approximation to the self-energy of composite bosons.

To generalize the above results to a “dilute” system of *composite* bosons, it is essential to take into account the *frequency dependence* of the effective two-boson interaction (2.11), which makes the summation over the frequencies inside the cycle somewhat more involved.

We first observe that from Eqs. (2.9) and (2.7) it follows that the “bare” propagator $\langle b^*(q)b(q) \rangle_{S_{\text{eff}}^{(2)}}$ can be written in the form:

$$\langle b^*(q)b(q) \rangle_{S_{\text{eff}}^{(2)}} = \frac{D(q)}{i\Omega_\nu - \left(\frac{\mathbf{q}^2}{4m} - \mu_B \right)}, \quad (3.1)$$

with the notation

$$D(q) = -\frac{\beta}{\mathcal{V}} \frac{4\pi}{m^2 a_F} \left(1 + \sqrt{1 + \frac{-i\Omega_\nu + \frac{\mathbf{q}^2}{4m} - \mu_B}{\epsilon_0}} \right). \quad (3.2)$$

The factor $D(q)$, which reflects the existence of the internal wave function for the composite bosons, has a cut (when $i\Omega_\nu$ is replaced by the complex frequency z) along the positive real axis for $\text{Re}(z) \geq -2\mu$.

It is convenient to transfer the factors $D(q)$ from the “bare” propagators to the effective two-boson interactions, which these propagators are joined to. Specifically, every propagator associated with an “internal” line of a diagram transfers a factor $\sqrt{D(q)}$ to each of the two interaction vertices it is joined to, while each propagator associated with one of the two “external” lines transfers one factor $\sqrt{D(q)}$ to the single interaction it is joined to and assigns the remaining factor $\sqrt{D(q)}$ as a proportionality factor to the “full” propagator, which the diagram is meant to represent. In this way, the “full” propagator acquires the same overall factor $D(q)$ of the “bare” propagator (3.1) and the effective two-boson interaction of Eq. (2.11) is multiplied by $\sqrt{D(q_1)}\sqrt{D(q_2)}\sqrt{D(q_3)}\sqrt{D(q_4)}$. We are then led to *rescaling* the effective two-boson interaction as follows:

$$2u_2(q_1 \dots q_4) \equiv \tilde{u}_2(q_1 \dots q_4) \times \sqrt{D(q_1)}\sqrt{D(q_2)}\sqrt{D(q_3)}\sqrt{D(q_4)} \quad (3.3)$$

with $\tilde{u}_2(q_1 \dots q_4)$ given by Eq. (2.11). [Note that the above definition accounts, in particular, for the difference between $\tilde{u}_2(0)$ and $u_2(0)$ in Eq. (2.12).] The sum over the common Matsubara frequency which runs along a generic cycle cannot be performed explicitly owing to the frequency dependence of the two-boson interaction $u_2(q_1, q_2, q_3, q_4)$. However, it can be readily verified that all the interaction vertices appear along the cycle with the dependence $u_2(q + q_j, q_a, q_b, q + q_{j-1})$ on the common four momentum q running along the cycle. From the explicit expressions for $D(q)$ and $\tilde{u}_2(q_1, q_2, q_3, q_4)$ [Eqs. (3.2) and (2.11), respectively] it can then be readily proved that, when the sum over the common Matsubara frequency is turned into a contour integration over the complex frequency z , each factor u_2 has a *cut* along the positive real axis for $\text{Re}(z) \geq -\mu$.

It is thus clear that the contribution to the frequency sum coming from the singularities due to the frequency dependence of the bosonic potentials is strongly suppressed by the presence of the Bose factor $(e^{\beta z} - 1)^{-1}$ therein, since $\beta|\mu| \gg 1$ in the strong-coupling limit. In this limit, the contribution of these singularities can thus be neglected, with the result that the cycle is again proportional to the bosonic density ρ_B , by the very argument holding for pointlike bosons.

We conclude that, for a system of composite bosons in the ‘‘low-density’’ limit, the leading diagrams contain just *one cycle*, like the ones shown in Fig. 7(b). In analogy with the corresponding diagrams of Fig. 7(a) for pointlike bosons, we shall refer to these diagrams as the *T-matrix approximation for composite bosons*.

$$\bar{u}_2(q_1 \dots q_4) = \frac{1}{\beta\mathcal{V}} \sum_k \frac{1}{\epsilon(-k)\epsilon(k+q_2)\epsilon(-k+q_1-q_4)\epsilon(k+q_4)}. \quad (3.7)$$

With the above expression for the ‘‘full’’ particle-particle ladder, we can obtain the fermionic self-energy of interest in analogy to Eq. (2.17), by joining the incoming and outgoing arrows of the particle-particle ladder Γ with a single-particle fermionic Green’s function in the only possible way. We then write

$$\Sigma_F(k) = -\frac{1}{\beta\mathcal{V}} \sum_{k'} \Gamma(k+k')\mathcal{G}^0(k') \quad (3.8)$$

with Γ given by Eq. (3.4) and where \mathcal{G}^0 is the ‘‘bare’’ single-particle fermionic Green’s function. The self-energy (3.8) has in turn to be inserted into the fermionic Dyson’s equation, to yield the full single-particle fermionic Green’s function \mathcal{G} . Eventual extrapolation from the strong- to the weak-coupling limit through the crossover region requires us to eliminate the chemical potential in favor of the particle density ρ , by evaluating

B. Coupled equations defining the generalized *T*-matrix approximation for the BE-BCS crossover

Once the self-energy diagrams for composite bosons in the ‘‘low-density’’ limit have been selected according to the above prescriptions, there remains to determine the analytic expression of these diagrams. To this end, it is convenient to stick with the bosonic representation and write down the expression for the bosonic propagator $\langle b^*(q)b(q) \rangle_{S_{\text{eff}}}$ with the self-energy insertions of Fig. 7(b), making use of the standard bosonic diagrammatic rules.^{22,23}

Our ‘‘full’’ bosonic propagator is given by Dyson’s equation:

$$\Gamma^{-1}(q) = \Gamma_0^{-1}(q) - \Sigma_B^{(t)}(q), \quad (3.4)$$

where the quantity

$$\Sigma_B^{(t)}(q) = -\frac{2}{\beta\mathcal{V}} \sum_{q'} \Gamma_0(q') \bar{t}_B(q', q, q, q') \quad (3.5)$$

represents the *T*-matrix approximation to the self-energy for composite bosons. The bosonic *T*-matrix is, in turn, defined by the following integral equation:

$$\begin{aligned} \bar{t}_B(q_1, q_2, q_3, q_4) &= \bar{u}_2(q_1, q_2, q_3, q_4) \\ &\quad - \frac{1}{\beta\mathcal{V}} \sum_{q_5} \bar{u}_2(q_1, q_2, q_5, q_1 + q_2 - q_5) \\ &\quad \times \Gamma_0(q_5) \Gamma_0(q_1 + q_2 - q_5) \bar{t}_B(q_1 + q_2 - q_5, q_5, q_3, q_4), \end{aligned} \quad (3.6)$$

where \bar{u}_2 is proportional to the effective two-boson interaction of Eq. (2.11):

$$\rho = \frac{2}{\beta\mathcal{V}} \sum_k e^{i\omega_n \eta} \mathcal{G}(k), \quad (3.9)$$

where η is a positive infinitesimal.

Besides the explicit \mathcal{G}^0 in Eq. (3.8), also *all* single-particle fermionic Green’s functions entering the expression (3.4) for Γ are meant to be ‘‘bare’’ ones, in analogy to the original approach by Galitskii.²⁷ We expect, in fact, that, contrary to a statement made in Ref. 7, the inclusion of self-consistency in the explicit single-particle fermionic Green’s function of Eq. (3.8) should not be essential to represent correctly the fermionic self-energy, either in the strong-coupling limit (where, on physical grounds, it is rather the bosonic propagator that needs to be represented correctly) or in the weak-coupling limit (where self-consistency drops out anyway for a ‘‘low-density’’ Fermi system).

By the same token, inclusion of self-consistency in the single-particle fermionic Green’s functions entering the ex-

pression (3.4) for Γ would yield contributions of higher order in the small parameter $k_F a_F$ with respect to the ones retained (both in the weak- and strong-coupling limits).

Our theory, which by construction correctly describes in the strong-coupling limit a system of ‘‘low-density’’ composite bosons, reduces to the standard Galitskii’s approximation⁵ in the weak-coupling limit. In this way, both weak- and strong-coupling limits are treated correctly. Indeed, since in the weak-coupling limit the bare particle-particle ladder Γ_0 becomes proportional to a_F , we can estimate the order in $k_F a_F$ of a given diagram contributing to the ‘‘full’’ particle-particle ladder Γ , by counting the powers of a_F in terms of the number of ‘‘bare’’ ladders Γ_0 and the powers of k_F in terms of the dimensionality of the four-vector sums over products of internal single-particle fermionic Green’s functions (which can safely be done because all sums are convergent). By this procedure, we obtain that, in the weak-coupling limit, a diagram for Γ with L bosonic interaction vertices is smaller by a factor $(k_F a_F)^{2L}$ with respect to the ‘‘bare’’ ladder Γ_0 . The leading diagram for the fermionic self-energy will be thus obtained by closing the ‘‘bare’’ ladder Γ_0 with a bare fermionic Green’s function, which corresponds to Eq. (3.8) with Γ_0 in the place of Γ . As our bosonic T -matrix corrections to Γ_0 contain at least one bosonic interaction vertex, they will become irrelevant in the weak-coupling limit, being smaller at least by a factor $(k_F a_F)^2$ compared to the bare Γ_0 . Our Γ thus reduces to Γ_0 in the weak-coupling limit, and we fully recover Galitskii’s theory.

These considerations also prove that diagrams of the same order in $\rho_B^{1/3} a_B$ in the bosonic (strong-coupling) limit correspond to *different* orders in $k_F a_F$ in the fermionic (weak-coupling) limit; accordingly, they would have been dismissed as being irrelevant, if the selection of diagrams would have been made directly for the weak-coupling limit.

A complete numerical evaluation of Eqs. (3.7)–(3.9) exceeds the purposes of the present paper. In the next section we calculate the scattering length for composite bosons in the strong-coupling limit, as a degenerate case of the T -matrix given by Eq. (3.6). This calculation will ensure us that the diagrams of Fig. 7(b), beyond first order in the interaction potential for composite bosons, give contributions of the *same order* of magnitude as the first-order (Hartree-Fock) diagram. In addition, it will turn out that the series of diagrams depicted in Fig. 7(b) does *not* converge, making any truncation of the series not appropriate. For this reason, it is essential to solve the complete integral equation associated with this series of diagrams to get a correct description of the strong-coupling limit.

IV. NUMERICAL RESULTS FOR THE SCATTERING LENGTH OF COMPOSITE BOSONS

In three dimensions the *scattering length* a characterizes the low-energy collisions for the scattering from an ordinary potential. For the mutual scattering of two particles (each of mass M), a can be expressed by the relation $t(0) = 4\pi a/M$ in terms of the ordinary T matrix $t(0)$ in the limit of vanishing wave vector. In particular, within the Born approximation $t(0)$ is replaced by the Fourier transform $u(0)$ of the interparticle potential for the vanishing wave vector.

In a similar way, we *define* the scattering length a_B for composite bosons (each of mass $2m$) in the strong-coupling limit and for vanishing density, by setting $t_B(0) = 4\pi a_B/(2m)$, where $t_B(0) = [8\pi/(m^2 a_F)]^2 \bar{t}_B(0)$ and $\bar{t}_B(0) \equiv \bar{t}_B(0,0,0,0)$ [cf. Eqs. (2.12), (2.11), and (3.7)]. This quantity is expected to be important for the calculation of the bosonic self-energy (3.5), insofar as the generalized T matrix for composite bosons therein depends weakly on its arguments.

To lowest order in the effective interaction for composite bosons, we can replace $t_B(0)$ by $u_2(0)$ and write $u_2(0) = 4\pi a_B^{\text{Born}}/(2m)$, within the Born approximation. Comparison with Eq. (2.13) yields then the value $a_B^{\text{Born}} = 2a_F$, as anticipated by Eq. (2.14). This Born *approximation* to the scattering length was erroneously identified as the *exact* bosonic scattering length in Ref. 7.

In order to obtain the exact value of $\bar{t}_B(0)$ (and hence of the scattering length a_B), it is convenient to determine first the auxiliary quantity $\bar{t}_B(q, -q, 0, 0)$ by solving the following *closed-form* equation:

$$\begin{aligned} \bar{t}_B(q, -q, 0, 0) &= \bar{u}_2(q, -q, 0, 0) \\ &- \frac{1}{\beta V} \sum_{q'} \bar{u}_2(q, -q, q', -q') \Gamma_0(q') \\ &\times \Gamma_0(-q') \bar{t}_B(q', -q', 0, 0), \end{aligned} \quad (4.1)$$

which is obtained from Eq. (3.6) by setting $q_1 = -q_2 = q$ and $q_3 = q_4 = 0$. This integral equation can be solved by standard numerical methods, e.g., by reverting it to the solution of a system of coupled linear equations.

Before embarking into this numerical calculation, we can obtain a preliminary estimate of the value of $\bar{t}_B(0)$ with limited effort, by neglecting the four-vector dependence of \bar{t}_B as well as the frequency dependence of \bar{u}_2 on the right-hand side of Eq. (4.1). We thus write approximately

$$\begin{aligned} \left(\frac{\bar{t}_B(0)}{\bar{u}_2(0)} \right)^{-1} &= \left(\frac{t_B(0)}{u_2(0)} \right)^{-1} \\ &\simeq 1 + \int \frac{d\mathbf{q}}{(2\pi)^3} \bar{u}_2(\mathbf{q}, -\mathbf{q}, 0, 0) \frac{1}{\beta} \\ &\times \sum_{\Omega_\nu} \Gamma_0(q) \Gamma_0(-q) \\ &= 1 - \int \frac{d\mathbf{q}}{(2\pi)^3} u_2(\mathbf{q}, -\mathbf{q}, 0, 0) \frac{1}{\beta} \\ &\times \sum_{\Omega_\nu} \frac{1}{i\Omega_\nu - \frac{\mathbf{q}^2}{4m}} \frac{1}{i\Omega_\nu + \frac{\mathbf{q}^2}{4m}} \\ &= 1 + \int \frac{d\mathbf{q}}{(2\pi)^3} u_2(\mathbf{q}, -\mathbf{q}, 0, 0) \frac{2m}{\mathbf{q}^2}, \end{aligned} \quad (4.2)$$

where the last result holds to the leading order in the density. Recalling further from Ref. 15 that

$$u_2(\mathbf{q}, -\mathbf{q}, 0, 0) = u_2(0) \frac{4}{4 + (|\mathbf{q}|a_F)^2} \quad (4.3)$$

in the strong-coupling limit, we obtain for the integral on the right-hand side of Eq. (4.2) the following value (in three dimensions)

$$\int \frac{d\mathbf{q}}{(2\pi)^3} u_2(\mathbf{q}, -\mathbf{q}, 0, 0) \frac{2m}{q^2} = u_2(0) \frac{m}{\pi a_F} = 4, \quad (4.4)$$

where use has been made of the result (2.13). We thus obtain

$$\frac{a_B}{a_B^{\text{Born}}} = \frac{t_B(0)}{u_2(0)} \approx \frac{1}{5}, \quad (4.5)$$

which implies that the contribution of the series diagrams depicted in Fig. 7(b) is of the *same order of magnitude* as the contribution of the first-order (Hartree-Fock) diagram therein.

The above approximate calculation suggests us to consider in more detail the scattering problem for two true bosons (each of mass M), mutually interacting via a potential of the form (4.3), namely,

$$u(\mathbf{q}) = \frac{8\pi a_F}{M} \frac{\gamma}{1 + \tilde{q}^2/4}, \quad (4.6)$$

where $\tilde{q} = |\mathbf{q}|a_F$ and γ is a dimensionless coupling constant [$\gamma = 1$ and $M = 2m$ for the potential (4.3)]. Solving for this simplified scattering problem will, in fact, be instructive to obtain the solution of the original scattering problem (4.1) for composite bosons, since it will (i) suggest a nontrivial approximation to be carried over to the original Eq. (4.1), and (ii) assess whether the region of interest ($\gamma \approx 1$) belongs to the perturbative or nonperturbative regime of the scattering integral equation.

To this end, we recall the equation satisfied by the T matrix for two-body scattering. In particular, it is sufficient to consider the following degenerate form

$$t(\mathbf{q}, 0) = u(\mathbf{q}) - \int \frac{d\mathbf{q}'}{(2\pi)^3} \frac{u(\mathbf{q} - \mathbf{q}')t(\mathbf{q}', 0)}{\frac{q'^2}{M}}, \quad (4.7)$$

which resembles Eq. (4.1) for composite bosons but lacks its dependence on Matsubara frequencies. As already noted, the scattering length is related to $t(0) \equiv t(0, 0)$ by the relation $a = t(0)M/(4\pi)$. For a spherically symmetric potential, $t(\mathbf{q}, 0) = t(|\mathbf{q}|, 0)$ and the angular integral in Eq. (4.7) can be readily performed. The remaining integral over $|\mathbf{q}|$ can be suitably discretized over a mesh, until convergence is achieved for the desired value $t(0)$ (200 mesh points have proved sufficient to get a 1% accuracy in the scattering length).

The results for a (in units of a_F) vs γ are shown in Fig. 8, where the asterisks correspond to the numerical solution of Eq. (4.7) and the full curve represents the Born approximation $a^{\text{Born}}/a_F = 2\gamma$. Note that, in the region of interest ($\gamma \approx 1$), $a^{\text{Born}}/a \approx 3$ and the solution of Eq. (4.7) cannot be

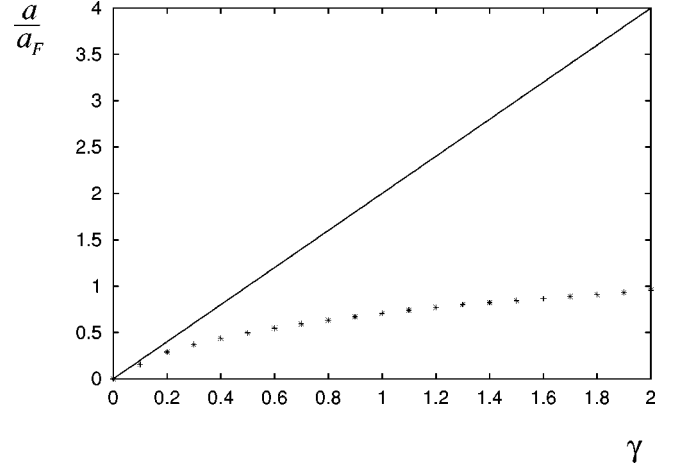


FIG. 8. Scattering length a (in units of a_F) vs the coupling strength γ of the potential (4.6), obtained by solving numerically the integral equation (4.7) (asterisks). The full line represents the Born approximation $a/a_F = 2\gamma$.

obtained by perturbative methods [the perturbative region—where the Born series associated with the integral equation (4.7) for a repulsive potential would converge—is, in fact, limited by $a^{\text{Born}}/a \leq 2$ and corresponds to $\gamma \leq 0.5$]. For this reason, any truncation of the integral equation would not be justified. Note also that the difference between a^{Born} and a increases drastically as γ increases (we have verified that a/a_F is proportional to $\log \gamma$ at least over eight decades).

Full numerical calculation of Eq. (4.1) requires us to introduce a finite-size mesh for the variables $(|\mathbf{q}|, \Omega)$ as well as $(|\mathbf{q}'|, \Omega')$, with the angular integral over \hat{q}' affecting only the function $\bar{u}_2(q, -q, q', -q')$. Equation (4.1) is thus reduced to a set of coupled equations for the unknowns $\bar{t}_B(|\mathbf{q}|, \Omega; |\mathbf{q}'|, -\Omega'; 0, 0)$, which we have solved by the standard Newton-Raphson algorithm with a linear interpolation for the integral over $|\mathbf{q}'|$ and Ω' . In this way we obtain

$$\frac{a_B}{a_B^{\text{Born}}} = \frac{\bar{t}_B(0)}{\bar{u}_2(0)} \approx \frac{1}{2.65} \quad (4.8)$$

within an estimated 5% numerical accuracy.

To verify that this result could not be inferred from a perturbative expansion of the integral equation (4.1), we calculate eventually the second term on the right-hand side of Eq. (4.1) by replacing $\bar{t}_B(q', -q', 0, 0)$ therein with $\bar{u}_2(q', -q', 0, 0)$ and by setting $q = 0$ everywhere for convenience. In this way we obtain

$$\begin{aligned} \bar{t}_B(0) &\approx \bar{u}_2(0) \left[1 - \frac{1}{\beta \mathcal{V}} \sum_{q'} \frac{\bar{u}_2(q', -q', 0, 0)^2}{\bar{u}_2(0)} \right. \\ &\quad \left. \times \Gamma_0(q') \Gamma_0(-q') + \dots \right] \\ &= \bar{u}_2(0) (1 - 1.69 + \dots), \end{aligned} \quad (4.9)$$

showing clearly that the geometric series would not converge in this case.

To summarize, we have shown that, in the strong-coupling limit, the value $a_B = 2a_F$ obtained for the composite-boson scattering length within the self-consistent fermionic T -matrix approximation,⁷ is modified to $a_B \simeq (3/4)a_F$ by the correct inclusion of *all* low-density contributions for a system of composite bosons.

V. CONCLUDING REMARKS

In this paper, we have determined the correct diagrammatic approximation for a “dilute” system of composite bosons, which form as tightly bound pairs of fermions in the limit of strong attraction between the constituent fermions. We have emphasized that it is physically the comparison of the average interparticle distance to the characteristic length associated with the *residual* interaction between the composite bosons to determine the “diluteness” condition in the strong-coupling limit of the original fermionic attraction. For this reason, it is essential to treat the residual interaction between the composite bosons with care, in order to control the strong-coupling limit of the theory appropriately. In this context, it is worth mentioning that the importance of a proper treatment of the residual boson-boson interaction in the strong-coupling limit has been emphasized in the pioneering paper by Nozières and Schmitt-Rink,³¹ but never duly taken into account in subsequent work.

We have also shown that the selection of the diagrammatic contributions according to the “diluteness” parameter proceeds along quite different lines in the weak-coupling limit (where the small parameter is $k_F a_F$) and in the strong-coupling limit (where the small parameter is $\rho_B^{1/3} a_B$). Accordingly, diagrammatic contributions of the *same* order in $\rho_B^{1/3} a_B$ in the strong-coupling limit correspond, in general, to *different* powers of $k_F a_F$ in the weak-coupling limit.

Our selection of diagrammatic contributions has rested on a suitable regularization of the fermionic interaction, which has caused the ratio between the particle-particle and particle-hole contributions to be infinite. For a Hubbard Hamiltonian on a lattice, where this regularization cannot be applied, we expect the difference between particle-particle and particle-hole contributions to be less extreme albeit still appreciable, so that our selection of diagrammatic contributions may still remain valid.

Quite generally, we have remarked that, with our choice of the fermionic interaction, the most general structure of the diagrammatic theory is constructed with the “bare” particle-particle ladder plus an infinite set of (four, six, . . . , n -point) vertices. This remains true for *any* value of the fermionic coupling and not just in the strong-coupling limit where the composite bosons form. We have also remarked that the “diluteness” parameter ($k_F a_F$ or $\rho_B^{1/3} a_B$) emerges *naturally* from the theory, both in the weak- and strong-coupling limits, without having to be imposed as an external condition.

Accordingly, keeping track of the powers of this small parameter in the diagrammatic theory can be relevant *only* in the weak- and strong-coupling limits. In the intermediate-coupling (crossover) region, on the other hand, a small parameter is lacking and consequently the diagrammatic approximations cannot be controlled by any means.

For these reasons, implementing the self-consistency of the fermionic Green’s functions within the fermionic T -matrix approximation⁷ does not seem *a priori* to be an important issue for the BCS-BE crossover. Self-consistency, in fact, drops out in the weak- and strong-coupling limits when the “diluteness” parameter is small, while in the intermediate (crossover) region inclusion of self-consistency within the fermionic T -matrix approximation (as well as within any other approximation over and above it) *cannot anyway be controlled* by the lack of a small parameter (even though inclusion of self-consistency might produce in practice sizable numerical effects).

We have emphasized in this paper that the (self-consistent) fermionic T -matrix approximation does not account properly for the boson-boson interaction in the strong-coupling limit, at least in *three* dimensions. This approximation, however, has been recently adopted to discuss pseudogap and related issues within the negative- U Hubbard model in *two* dimensions.^{32–34} Assessing to what extent the approach we have developed in this paper can be carried over to the two-dimensional case is not *a priori* evident and will require further investigations. From physical intuition one would expect the bosonic regime to be reached even more effectively in two than in three dimensions, insofar as the two-fermion bound state is present in two dimensions for any (attractive) coupling strength. Our dealing with the three-dimensional case first was required for manifesting at the outset the effects on the BCS-BE crossover due to the progressive formation of bound-fermion pairs, thus isolating them from other effects which are peculiar to the two-dimensional case.

It is finally interesting to point out the strong analogy between the present treatment of the BCS to BE crossover in a condensed-matter system and the so-called Otsuka-Arima-Iachello mapping introduced some time ago in nuclear physics,^{35,36} where a systematic mapping between the diagrammatic theories for (composite) bosons and (constituent) fermions was also provided, albeit in a quite different physical context and with the use of approximations more specific to the nuclear problem.

ACKNOWLEDGMENTS

We are indebted to C. Castellani, C. Di Castro, M. Grilli, F. Iachello, V. Janiš, A. Perali, and F. Pistolesi for helpful discussions. P.P. gratefully acknowledges financial support from the Italian INFN under Contract No. PRA-HTCS/96-98.

*Electronic address: pieri@str.unicam.it

†Electronic address: strinati@camars.unicam.it

¹Y. J. Uemura *et al.*, Phys. Rev. Lett. **62**, 2317 (1989).

²H. Ding *et al.*, Nature (London) **382**, 51 (1996); Phys. Rev. Lett. **78**, 2628 (1997).

³A. G. Loeser *et al.*, Science **273**, 325 (1996).

⁴V. Janiš, J. Phys.: Condens. Matter **10**, 2915 (1998).

⁵V. M. Galitskii, Zh. Éksp. Teor. Fiz. **34**, 151 (1958) [Sov. Phys. JETP **7**, 104 (1958)].

⁶S. T. Beliaev, Zh. Éksp. Teor. Fiz. **34**, 433 (1958) [Sov. Phys. JETP **7**, 299 (1958)].

⁷R. Haussmann, Z. Phys. B: Condens. Matter **91**, 291 (1993).

- ⁸R. Frésard, B. Glaser, and P. Wölfle, *J. Phys.: Condens. Matter* **4**, 8565 (1992).
- ⁹R. Micnas *et al.*, *Phys. Rev. B* **52**, 16 223 (1995).
- ¹⁰B. Jankó, J. Maly, and K. Levin, *Phys. Rev. B* **56**, R11 407 (1997).
- ¹¹J. R. Engelbrecht, A. Nazarenko, M. Randeria, and E. Dagotto, *Phys. Rev. B* **57**, 13 406 (1998).
- ¹²B. Kyung, E. G. Klepfish, and P. E. Kornilovitch, *Phys. Rev. Lett.* **80**, 3109 (1998).
- ¹³In the *extreme* strong-coupling limit, the interaction between the composite bosons is bound to vanish (cf. Refs. 7,15). Physically, this is due to the fact that, for a point-contact interaction between the constituent fermions, the composite bosons of size a_F mutually interact only when overlapping. For this reason, the bosonic scattering length a_B should be proportional to a_F . The condition $k_F a_F \ll 1$ can then be interpreted as $\rho_B^{1/3} a_B \ll 1$, which is the “diluteness” condition for a Bose gas. The “diluteness” condition thus emerges naturally both in the weak- and strong-coupling limits, and should *not* be imposed as an additional condition on the system.
- ¹⁴C. A. R. Sá de Melo, M. Randeria, and J. R. Engelbrecht, *Phys. Rev. Lett.* **71**, 3202 (1993).
- ¹⁵F. Pistolesi and G. C. Strinati, *Phys. Rev. B* **53**, 15 168 (1996).
- ¹⁶S. Stintzing and W. Zwerger, *Phys. Rev. B* **56**, 9004 (1997).
- ¹⁷Already at the mean-field level, the exact solution available for a contact potential [M. Marini, F. Pistolesi, and G. C. Strinati, *Eur. Phys. J. B* **1**, 151 (1998)] shows that approximations valid on the BE side extrapolate well to the BCS side, but not vice versa.
- ¹⁸Throughout this paper, by the bosonic Hartree-Fock approximation we mean the self-energy diagram of lowest order in the (symmetrized) bosonic interaction, which has the *same* topological structure of the bosonic Hartree-Fock self-energy diagram but lacks the self-consistency in the bosonic propagator.
- ¹⁹The choice of the “contact” potential (2.2) does not allow the fermionic attraction to extend over a *finite* range. If a finite-range fermionic attraction would instead have been adopted, the effective boson-boson potential in the strong-coupling limit would acquire an *attractive* part which would dominate over the usual repulsive part due to Pauli principle, in the sense that the bosonic scattering length associated with the attractive part would not vanish in that limit. The attractive part would thus lead to an instability of the bosonic system when the finite-range fermionic attraction gets sufficiently strong. To avoid this instability, a condition of the type $\epsilon_0 \ll k_0^2/(2m)$ has to be imposed on the BE limit, where k_0 is the wave vector specifying the finite range of the potential and ϵ_0 is the bound-state energy of the two-body problem [cf. footnote 43 of Ref. 15]. In this context, it is worth mentioning the recent work by G. Röpke *et al.* [*Phys. Rev. Lett.* **80**, 3177 (1998)] where it has been shown that, in the strong-coupling limit, there exists a competition between pair and quartet condensation in a Fermi liquid with finite-range attraction. It is then clear that adopting a finite-range fermionic potential merely makes the BCS-BE crossover more involved, and it is thus not relevant to the purposes of the present paper.
- ²⁰S. Hikami, *Phys. Rev. B* **24**, 2671 (1981).
- ²¹A precise definition of what is meant by “weak-” and “strong-” coupling limits is in order at this point. In the weak-coupling limit, we let a_F vanish while keeping the density ρ and the temperature T *finite*. In the strong-coupling limit, on the other hand, we let the binding energy ϵ_0 go to infinity, for given values of ρ and T . For vanishing ρ , we expect the chemical potential to approach $-\epsilon_0/2$ on physical grounds. Corrections to this value due to finite density and temperature effects are further expected to be negligible, provided $\rho^{2/3}/(2m) \ll \epsilon_0$ and $T \ll \epsilon_0$. Both conditions are met when $\epsilon_0 \rightarrow \infty$, yielding $\beta\mu \rightarrow -\infty$ in the strong-coupling limit.
- ²²V. N. Popov, *Functional Integrals in Quantum Field Theory and Statistical Physics* (Riedel, Dordrecht, 1983).
- ²³V. N. Popov, *Functional Integrals and Collective Excitations* (Cambridge University Press, Cambridge, 1987).
- ²⁴Note that $u_2(0)$ is *positive* in the strong-coupling limit, thus ensuring the *stability* of the bosonic system.
- ²⁵It can be readily verified that, if at least one (2l)-point vertex enters a bosonic self-energy diagram, then there are at least (l - 1) bosonic cycles in that diagram (see also Ref. 30). Since each bosonic cycle gives a contribution proportional to the density ρ (as shown in Sec. III), four-point vertices only contribute to the bosonic self-energy to lowest order in ρ .
- ²⁶Cf., e.g., A. L. Fetter and J. D. Walecka, *Quantum Theory of Many-Particle Systems* (McGraw-Hill, New York, 1971).
- ²⁷Self-consistency gives contributions at least of order $(k_F a_F)^2$ to the fermionic self-energy. For this reason, it was not considered by Galitskii in the calculation of the self-energy to order $k_F a_F$ (Ref. 5). A first round of self-consistency was, however, included by Galitskii in the calculation of the self-energy of a “dilute” Fermi gas to order $(k_F a_F)^2$. In the context of the BCS-BE crossover, the complete self-consistency within the fermionic T -matrix approximation has been considered only recently (cf. Refs. 8 and 7), and since then utilized by several authors in this field (Refs. 9, 11, and 12).
- ²⁸G. Baym and L. P. Kadanoff, *Phys. Rev.* **124**, 287 (1961).
- ²⁹G. Baym, *Phys. Rev.* **127**, 1391 (1962).
- ³⁰In the context of the “dilute” Bose gas the term “cycle” has a specific meaning, different from the term “loop” utilized in field theory in the context of the loop expansion (Ref. 23). By a “cycle” we mean, in fact, a sequence of bosonic propagators arranged in a closed path, with *all arrows running in the same direction* and with a common four-momentum integration for all propagators.
- ³¹P. Nozières and S. Schmitt-Rink, *J. Low Temp. Phys.* **59**, 195 (1985).
- ³²J. J. Deisz, D. W. Hess, and J. W. Serene, *Phys. Rev. Lett.* **80**, 373 (1998).
- ³³J. R. Engelbrecht and A. Nazarenko, Cond-mat/9806223 (unpublished).
- ³⁴P. E. Kornilovitch and B. Kyung, *J. Phys.: Condens. Matter* **11**, 741 (1999).
- ³⁵T. Otsuka, A. Arima, and F. Iachello, *Nucl. Phys. A* **309**, 1 (1978).
- ³⁶F. Iachello and I. Talmi, *Rev. Mod. Phys.* **59**, 339 (1987).